Mechanical Properties and Rapid Low-temperature Consolidation of Nanocrystalline Cu-ZrO$_2$ Composites by Pulsed Current Activated Heating

Bo-Ram Kang[1], Jin-kook Yoon[2], Kyung-Tae Hong[2], and In-Jin Shon[1,*]

[1]Division of Advanced Materials Engineering, the Research Center of Advanced Materials Development, Chonbuk National University, 664-14 Deokjin-dong 1-ga, Deokjin-gu, Jeonju, Jeonbuk 561-756, Korea
[2]Materials Architecturing Research Center, Korea Institute of Science and Technology, PO BOX 131, Cheongryang, Seoul 130-650, Korea

Metal-ceramic compositr can be obtained with an optimum combination of low density, high oxidation resistance, and high hardness of the ceramic and toughness of the metal. Therefore, metal matrix composites are recognized as candidates for aerospace, automotive, biomaterials, and defense applications. Despite its many attractive properties, the low fracture toughness of ZrO$_2$ limits its wide application. One of the most obvious tactics to improve the mechanical properties has been to fabricate a nanostructured material and composite material. Nano-powders of Cu and ZrO$_2$ were synthesized from 2CuO and Zr powders by high-energy ball milling. Nanocrystalline 2Cu-ZrO$_2$ composite was consolidated within 5 minutes from mechanically synthesized powders of ZrO$_2$ and 2Cu at low temperature, by a pulsed current activated sintering method. The relative density of the composite was 98.5%. The fracture toughness of 2Cu-ZrO$_2$ composite in this study is higher than that of monolithic ZrO$_2$, without great decrease of hardness.

Keywords: powder processing, composites, sintering, nanostructured materials, mechanical properties

1. INTRODUCTION

Metal-ceramic composite can be obtained with an optimum combination of low density, high oxidation resistance, and high hardness of the ceramic and toughness of the metal. Therefore, metal matrix composites are recognized as candidates for aerospace, automotive, biomaterials, and defense applications.

ZrO$_2$ has a density of 5.98 g cm^{-3}, a Young's modulus of 210 GPa, excellent oxidation resistance, and good high-temperature mechanical properties [1,2]. Cu has a density of 8.9 g cm^{-3}, a Young's modulus of 130 GPa, and good fracture toughness [2]. Hence, microstructure consisting of Cu and ZrO$_2$ may be able to satisfy the requirements of good oxidation resistance and high mechanical properties of successful structural materials.

Nanocrystalline materials have received much attention as advanced engineering materials with improved physical and mechanical properties [3,4]. As nanomaterials possess excellent mechanical properties (high strength, high hardness, excellent ductility, and toughness) more attention has undoubtedly been paid to the application of nanomaterials

[5,6]. In recent days, nanocrystalline powders have been developed by thermochemical and thermomechanical processes of spray conversion process (SCP), co-precipitation, electrical wire explosion, and high-energy milling [7-9]. The sintering temperature of high-energy mechanically milled powder is lower than that of unmilled powder, due to the increased reactivity, surface energies, and surface area of the milled powder, which contribute to its so-called mechanical activation [10-12]. However, the grain size in sintered materials becomes much larger than that in pre-sintered powders, due to fast grain growth during the conventional sintering process. Therefore, even though the initial particle size is less than 100 nm, during conventional sintering the grain size increases rapidly up to 2 μm or larger [13]. Therefore, controlling grain growth during sintering is one of the keys to the commercial success of nanostructured materials. In this regard, the pulsed current activated sintering method (PCASM), which can make dense materials within several minutes, has been shown to be effective in achieving this goal [14-16]. In addition, the spark plasma formed between the powder particles enhances the clean surface of the particles, and the rate of diffusion between the particles [17-20].

The purpose of this work is to produce dense nanocrystalline 2Cu-ZrO$_2$ composites within 5 minutes at low temperature from mechanically synthesized powders, under simultaneous

application of 1 GPa pressure, and a pulsed current, and to evaluate the microstructure and mechanical properties (hardness and fracture toughness) of the composites.

## 2. EXPERIMENTAL PROCEDURE

Powders of 99% CuO (< 5 μm, Aldrich) and 99.5% pure Zr (-325 mesh, Sejong) were used as starting materials. 2CuO and Zr powder mixtures were first milled in a high-energy ball mill, Pulverisette-5 planetary mill at 250 rpm for 10 h. Tungsten carbide balls (10 mm in diameter) were used in a sealed cylindrical stainless steel vial under argon atmosphere. The weight ratio of ball-to-powder was 30:1. Milling resulted in a significant reduction of grain size. The grain sizes of Cu and ZrO₂ were calculated by Suryanarayana and Grant Norton's formula [21].

After milling, the mixed powders were placed in a WC die (outside diameter, 35 mm; inside diameter, 5 mm; height, 40 mm), and then introduced into a pulsed current activated sintering system made by Eltek in South Korea. A schematic of this is shown in Ref. [14-16]. The four major stages in the synthesis are as follows. Stage 1 - Evacuation of the system. Stage 2 - Application of uniaxial pressure. Stage 3 - Heating of the sample by pulsed current (on time; 20 μs, off time; 10 μs). Stage 4 - Cooling of the sample. The process was carried out under a vacuum of 40 mtorr.

The relative densities of the sintered sample measured by the Archimedes method are over 98.5% of the theoretical value. Microstructural information was obtained from product samples, which were polished at room temperature. Compositional and micro structural analyses of the products were made through X-ray diffraction (XRD) with Cu target and scanning electron microscopy (SEM), with energy dispersive X-ray analysis (EDS). The Vickers hardness was measured by performing indentations at a load of 10 kg, and a dwell time of 15s on the sintered samples.

3. RESULTS AND DISCUSSION

Figure 1 shows Gibbs free energy of formation of 2Cu+ZrO₂ from 2CuO+Zr. The values is negative in all temperature range. Therefore, the interaction between 2CuO and Zr, i.e.,

$$2CuO + Zr \rightarrow 2Cu + ZrO_2 \qquad (1)$$
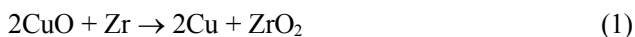
is thermodynamically feasible.

X-ray diffraction results of raw powder of CuO and Zr are shown in Fig. 2(a) and Fig. 2(b). Figure 2(c) shows X-ray diffraction result of high-energy ball milled powders for 10 h. The reactant powders of CuO and Zr were not detected, but the products, Cu and ZrO₂, were detected. From the above result, mechanical synthesis completely occurs during the high-energy ball milling. Figure 3 shows a plot of B_r ($B_{crystalline}$ +B_{strain}) cosθ versus sinθ of Cu and ZrO₂ in milled powders.
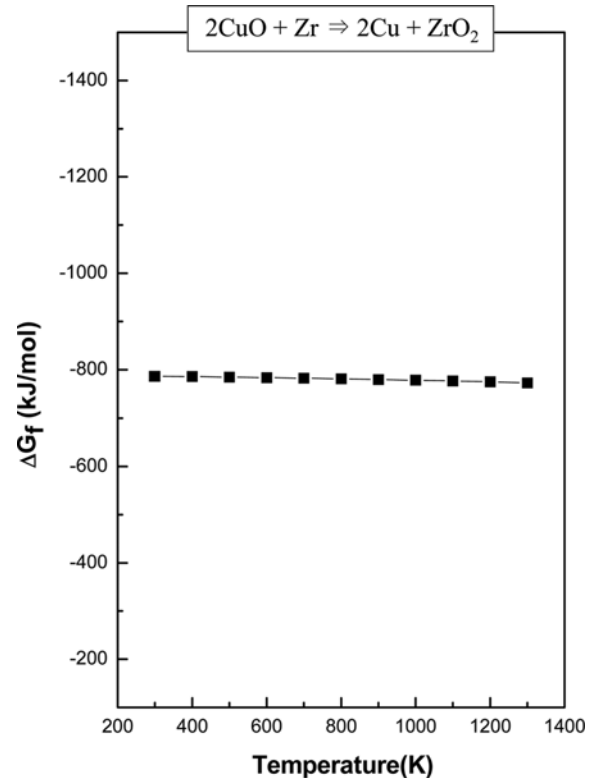

Fig. 1. Temperature dependence of Gibbs free energy variation by the interaction of 2CuO and ZrO₂.

The average grain sizes of Cu and ZrO₂ measured by Suryanarayana and Grant Norton's formula from XRD data are about 9 nm and 18nm, respectively. A scanning electron microscopy image and X-ray mapping of the milled powders are shown in Fig. 4. The powders are very fine, and the X-ray mapping results show that the products (Cu, ZrO₂) are uniformly distributed (Figs. 5(b), (c) and (d)). Gray phase and dark phase are Cu an ZrO₂ due to mass contrast, respectively.

The shrinkage displacement-time (temperature) curve provides useful information on the consolidation behavior. Figure 5 shows the variations in shrinkage displacement and temperature of the surface of the WC die with heating time, during the processing of the Cu and ZrO₂ system. As the pulsed current was applied, the shrinkage displacement continually increased with temperature, up to about 620 °C. Afterwards, they contract almost linearly to 630 °C, at which the consolidation terminates. The shrinkage curve suggests that the consolidation terminates in five minutes.

X-ray diffraction pattern of the sample heated to 630 °C is shown in Fig. 6. Only Cu and ZrO₂, were detected. The structure parameters, i.e. the average grain sizes of Cu and ZrO₂, obtained from the X-ray data by Suryanarayana and Grant Norton's formula [21], were 27 nm and 42 nm, respectively. Figure 7 shows a SEM image of the sample heated to 630 °C. From the figure, it is apparent that the grain sizes of Cu and
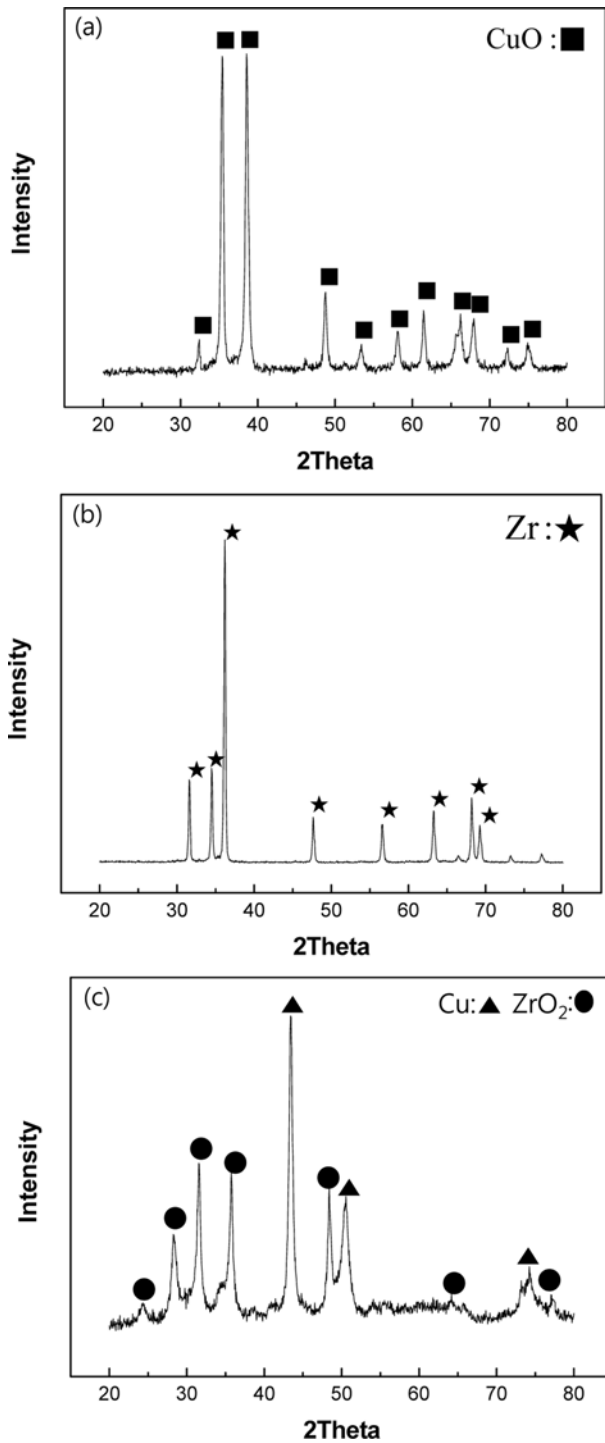
Fig. 2. XRD patterns of raw materials and mechanically synthesized powder: (a) CuO, (b) Zr, and (c) mechanically synthesized powder.

Fig. 3. Plot of sinθ versus $B_r \cos\theta$ for (a) Cu and (b) ZrO_2 in mechanically milled powders.

Fig. 4. Scanning electron microscopy image and X-ray mapping of Cu and ZrO_2 powders: (a) SEM image, (b) O mapping, (c) Cu mapping, and (d) Zr mapping.

ZrO_2 consist of nanocrystallites. Thus, the average grain sizes of the sintered Cu and ZrO_2 are not much larger than those of the initial powders, indicating the absence of grain growth during sintering. This retention of the grain size is attributed to the rapid heating rate and the relatively short-term exposure of the powders to the high temperature. The corresponding relative
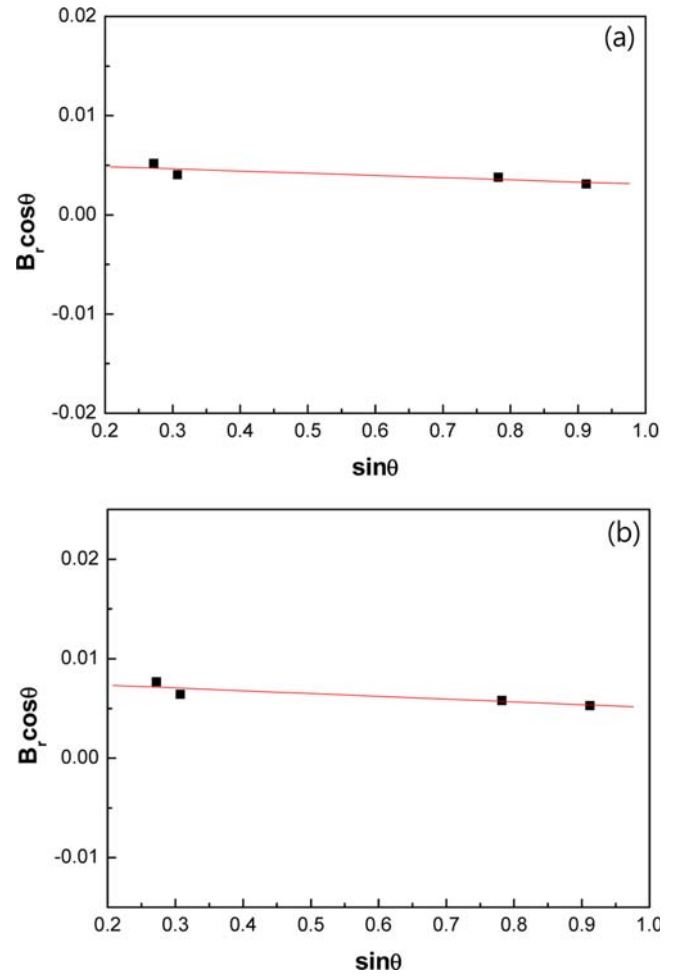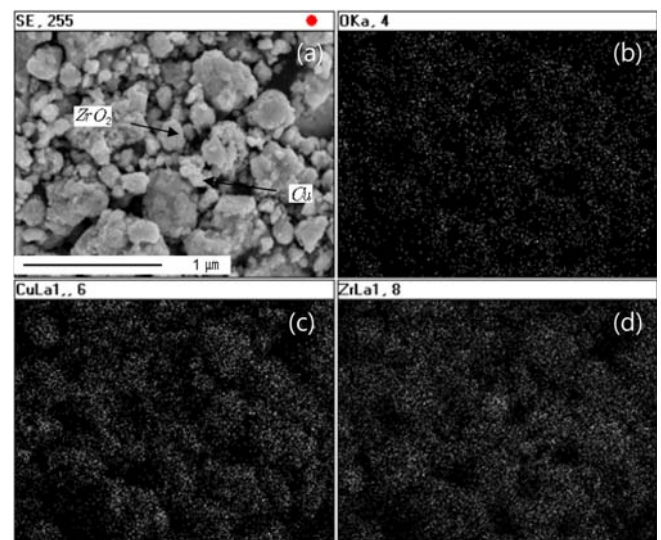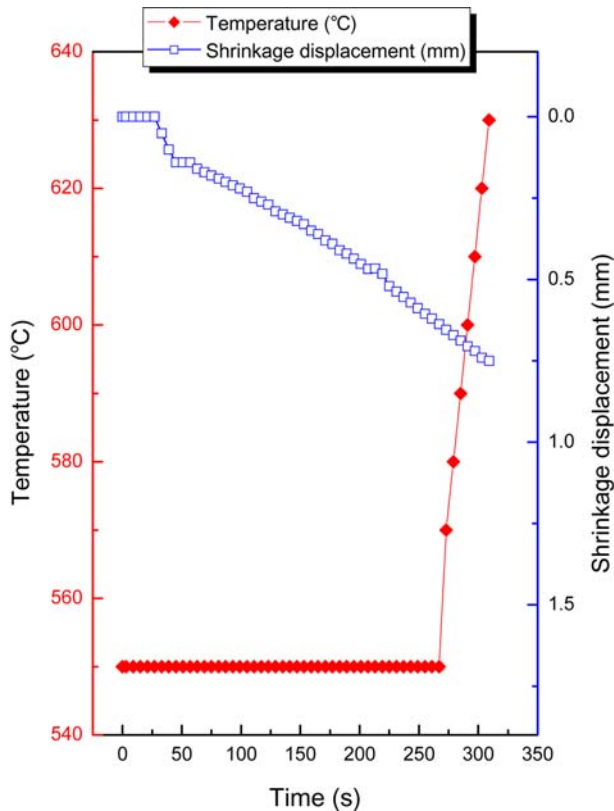
Fig. 5. Variation of temperature and shrinkage displacement with heating time, during pulsed current activated sintering of 2Cu + ZrO₂.
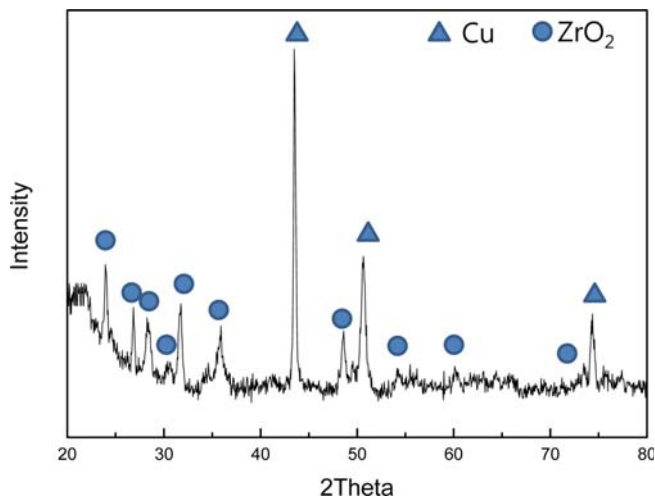

Fig. 6. XRD patterns of the 2Cu-ZrO₂ composite sintered to 630 °C.

density was approximately 98.5%.

The role of the pulsed current in sintering has been the focus of several attempts to provide an explanation of the observed sintering enhancement, and the improved properties of the products. The role played by the pulsed current has been variously explained. The effect has been explained by rapid heating due to Joule heating at contacts points, the surface cleaning
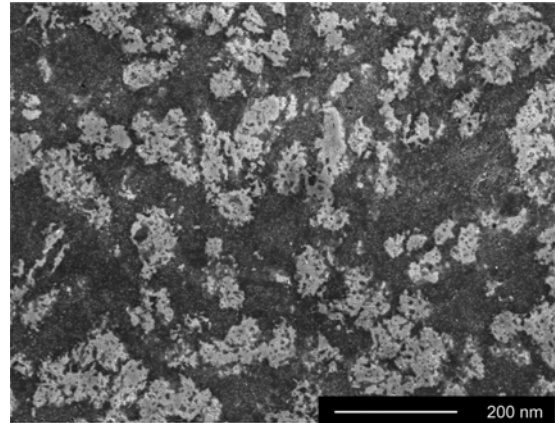

Fig. 7. FE-SEM image of the 2Cu-ZrO₂ composite sintered to 630 °C.

due to presence of plasma in pores separating powder particles, and the contribution of the current to fast mass transport [17-20,22].

Vickers hardness measurements were made on polished sections of the 2Cu-ZrO₂ composite, using a 10 kg$_f$ load and 15 s dwell time. The calculated hardness value of 2Cu-ZrO₂ composite was 390 kg/mm^2. This value represents an average of five measurements. Indentations with large enough loads produced median cracks around the indent. From the length of these cracks, fracture toughness values can be calculated using two expressions. The first expression, proposed by Anstis *et al.* [23], is

$$K_{IC} = 0.016 \, (E/H)^{1/2} \cdot P/C^{3/2} \tag{3}$$

where, E is Young's modulus, H is the indentation hardness, P is the indentation load, and C is the trace length of the crack measured from the center of the indentation. The modulus was calculated by the rule mixtures for the 0.75 volume fraction of ZrO₂ and the 0.25 volume fraction of Cu, using E(ZrO₂) = 207 GPa [1], and E(Cu) = 128 GPa [2].

The second expression, proposed by Niihara *et al.* [24], is

$$K_{IC} = 0.023 \, (c/a)^{-3/2} \cdot H_v \cdot a^{1/2} \tag{3}$$

where, *c* is the trace length of the crack measured from the center of the indentation, *a* half of the average length of two indent diagonals, and H_v the hardness. As in the case of hardness values, the toughness values were derived from the average of five measurements. The toughness values obtained by the two methods of calculation are 4.8 and 4.5 MPa·m$^{1/2}$, respectively. Indentations with large enough loads produced median cracks around the indent. The hardness and fracture toughness of ZrO₂ with grain size of 67nm and relative density of 94%, which was sintered at 1100 °C under 80 MPa, are reported as 400 kg/mm^2 and 3.5 MPa·m$^{1/2}$, respectively [25]. In this study, higher relative density of 2Cu-ZrO₂ composite
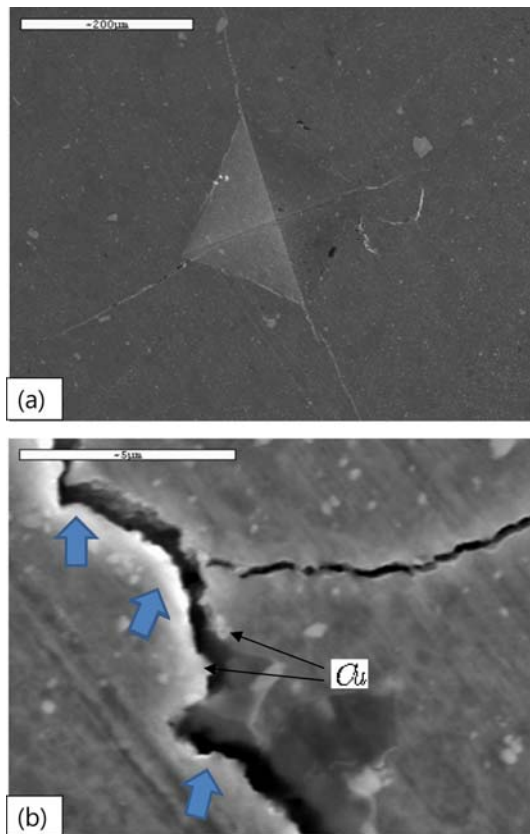
Fig. 8. (a) Vickers hardness indentation and (b) crack propagation, in the 2Cu-ZrO$_2$ composite sintered to 630 °C.

was obtained at low temperature (630 °C), due to applying very high pressure (1 GPa). Applying pressure during sintering adds another term to the surface energy driving force, such that the total driving force, F$_D$, may be expressed as [26]:

$$F_D = \gamma + (P_a r/\pi), \tag{3}$$

where, γ is the surface energy, P_a is the applied pressure, and r is the particle radius. The effect of pressure on the densification of nanometric stabilized ZrO$_2$ during high frequency-induced heated sintering was investigated by Kim *et al*. [27]. The relative density significantly increased, as pressure increased from 60 to 100 MPa, for sintering at 1000 °C.

Comparing the hardness and fracture toughness values obtained in this study with those reported by others [25], the fracture toughness of 2Cu-ZrO$_2$ composite in this study is higher than that of monolithic ZrO$_2$ [25], without great decrease of hardness. To understand the mechanical properties of 2Cu-ZrO$_2$ composite, two factors may be considered. One is the effect of the relative density of product. The other would be the role of the second phase in crack propagation that affects the toughness. It is generally accepted that high relative density and the addition of the ductile phase may increase the fracture toughness, according to the crack dividing, deflecting, bowing, and branching effect. The Vickers hard-

ness indentations and crack propagation in 2Cu-ZrO$_2$ composite are shown in Fig. 8. They typically show cracks propagating radially from the indentation. The toughness of 2Cu-ZrO$_2$ composite may be that the Cu network may deter crack propagation. Figure 8(b) shows a crack propagating in a deflective and dividing manner ($\uparrow$), in 2Cu-ZrO$_2$ composite. The enhanced fracture toughness of 2Cu-ZrO$_2$ composite is believed to be as a result of the high relative density of the composite, and the Cu in the composite deterring the crack propagation.

4. CONCLUSIONS

Nanopowders of Cu and ZrO$_2$ are synthesized from 2CuO and Zr powders by high-energy ball milling. Using the pulsed current activated sintering method, the densification of nanocystalline ZrO$_2$ reinforced Cu composite was accomplished from mechanically synthesized powders. Complete densification could be achieved within a duration of 5 minutes at 630°C, under the high pressure of 1GPa. The relative density of the composite was 98.5%, for the applied pressure and pulsed current. The average grain sizes of Cu and ZrO$_2$ prepared by PCAS were about 27 nm and 42 nm, respectively. The average hardness and fracture toughness values obtained were 390 kg/mm^2 and 4.8 MPa·m$^{1/2}$, respectively.

The fracture toughness of 2Cu-ZrO$_2$ composite in this study is higher than that of monolithic ZrO$_2$, without decrease of hardness. The enhanced fracture toughness of 2Cu-ZrO$_2$ composite is believed to be due to the high relative density of the composite, and Cu in the composite deterring crack propagation.

REFERENCES

1. S. G. Huang, *J. European Ceramic Society* **27**, 3269 (2007).
2. S. G. Huang, *J. European Ceramic Society* **27**, 3269 (2007).
3. MS. El-Eskandarany, *J. Alloy. Compd.* **305**, 225 (2000).
4. L. Fu, L. H. Cao, and Y. S. Fan, *Scripta Mater.* **44**, 1061 (2001).
5. I.-J. Shon, *Korean J. Met. Mater.* **52**, 573 (2014).
6. S. Berger, R. Porat, and R. Rosen, *Prog. Mater. Sci.* **42**, 311 (1997).
7. I.-J. Shon, H.-S. Kang, J.-M. Doh, and J.-K. Yoon, *Mat. Sci. Eng. A* **606**, 139 (2014).
8. Z. Fang and J. W. Eason, *International Journal of Refractory Metals and Hard Materials,* **13**, 297 (1995).

9. S. Ni., Y. B. Wang, X. Z. Liao, S. N. Alhajeri, H. Q. Li, Y. H. Zhao, E. J. Lavernia, S. P. Ringer, T. G. Langdon, and Y. T. Zhu, *Mater. Sci. Eng. A* **528**, 3398 (2011).

10. F. Charlot, E. Gaffet, B. Zeghmati, F. Bernard, and J. C. Liepce, *Mater. Sci. Eng. A* **262**, 279 (1999).

11. I. J. Shon, K. I. Na, J. M. Doh, H. K. Park, and J. K. Yoon, *Met. Mater. Int.* **19**, 99 (2013).

12. I. J. Shon, G. W. Lee, J. M. Doh, and J. K. Yoon, *Electron. Mater. Lett.* **9**, 219 (2013).

13. J. Jung and S. Kang, *Scripta Mater.* **56**, 561 (2007).

14. G-W. Lee and I.-J. Shon, *Korean J. Met. Mater.* **51**, 95 (2013).

15. I. J. Shon, S.-L. Du, J.-M. Doh, and J.-K. Yoon, *Met. Mater. Int.* **19**, 1041 (2013).

16. I.-J. Shon, H.-G. Jo, and H. J. Kwon, *Korean J. Met. Mater.* **52**, 343 (2014).

17. Z. Shen, M. Johnsson, Z. Zhao, and M. Nygren, *J. Am. Ceram. Soc.* **85**, 1921 (2002).

18. J. E. Garay, U. Anselmi-Tamburini, Z. A. Munir, S. C. Glade, and P. Asoka-Kumar, *Appl. Phys. Lett.* **85**, 573 (2004).

19. J. R. Friedman, J. E. Garay. U. Anselmi-Tamburini, and Z. A. Munir, *Intermetallics*. **12**, 589 (2004).

20. J. E. Garay, U. Anselmi-Tamburini, and Z. A. Munir, *Acta Mater*. **51**, 4487 (2003).

21. C. Suryanarayana and M. Grant Norton, *X-ray Diffraction A Practical Approach*, p.213, Plenum Press, New York (1998).

22. R. Raj, M. Cologna, and J. S. C. Francis, *J. Am. Ceram. Soc*. **94**, 1941 (2011).

23. G. R. Anstis, P. Chantikul, B. R. Lawn, and D. B. Marshall, *J. Am. Ceram. Soc*. **64**, 533 (1981).

24. K. Niihara, R. Morena, and D. P. H. Hasselman, *J. Mater. Sci. Lett*. **1**, 12 (1982).

25. S.-M. Kwak, H.-K. Park, and I.-J. Shon, *Korean J. Met. Mater*. **51**, 341 (2013).

26. R. L. Coble, *J. Appl. Phys*. **41**, 4798 (1970).

27. H.-C. Kim, I.-J. Shon, I.-K. Jeong, I.-Y. Ko, *Met. Mater. Int*. **12**, 393 (2006).